

# All-optical production of ${}^7\text{Li}$ Bose-Einstein condensation using Feshbach resonances

Noam Gross and Lev Khaykovich

*Department of Physics, Bar-Ilan University, Ramat-Gan, 52900 Israel*

(Received 5 December 2007; published 4 February 2008)

We show an all-optical method of making  ${}^7\text{Li}$  condensates using the tunability of the scattering length in the proximity of a Feshbach resonance. We report the observation of two Feshbach resonances on the  $|F=1, m_F=0\rangle$  state. A narrow (broad) resonance of 7 G (34 G) width is detected at  $831 \pm 4$  G ( $884_{-13}^{+4}$  G). The position of the scattering length zero crossing between the resonances is found at  $836 \pm 4$  G. The broad resonance is shown to be favorable for runaway evaporation which we perform in a crossed-beam optical-dipole trap. Starting directly from the phase-space density of a magneto-optical trap we observe a Bose-Einstein condensation threshold in less than 3 s of forced evaporation.

DOI: [10.1103/PhysRevA.77.023604](https://doi.org/10.1103/PhysRevA.77.023604)

PACS number(s): 67.85.Hj, 34.50.Cx, 37.10.De

## I. INTRODUCTION

Achieving quantum degeneracy in ultracold atomic gases by all-optical means has become a well-accepted experimental technique because of several inherent advantages [1–7]. Optical traps allow strong confinement, resulting in high collision rates and rapid evaporative cooling. Confinement of arbitrary spin states and spin state mixtures is readily obtained. The possibility to tune interactions via Feshbach resonances usually requires optical trapping as they frequently occur in states that cannot be trapped magnetically [8,9]. Finally, large current coils needed for magnetic-field trapping that restrict optical access are avoided.

The first successful demonstration of an all-optically achieved  ${}^{87}\text{Rb}$  Bose-Einstein condensation (BEC) allowed a significant increase in the rate of BEC production and the resulting condensates were  $F=1$  spinors [1]. However, the main driving force behind the search for all-optical techniques was the need to condense specific atoms where “conventional” evaporation in the magnetic trap was not possible. Two prominent examples are spinless, and thus magnetically untrappable, BECs of Yb atoms achieved in a doubled YAG crossed dipole trap [2] and a BEC of  ${}^{133}\text{Cs}$  atoms [3] for which the strongly enhanced two-body losses from the magnetically trappable states prevent condensate formation in the “standard” way [10].

Although  ${}^7\text{Li}$  atoms can be evaporatively cooled in a magnetic trap [11], the task remains challenging due to several reasons. First,  ${}^7\text{Li}$  atoms possess a relatively small scattering length ( $a=-27a_0$ , where  $a_0$  is the Bohr radius) and a high two-body loss rate [12]. Second, the initial phase-space density is unfavorably limited by the absence of a polarization-gradient cooling mechanism. Third, since the scattering length drops with increased temperature and crosses zero at  $T=8$  mK [13], the use of adiabatic compression to increase the elastic collisional rate is ineffective. Therefore, the strong magnetic confinement needed to keep the evaporation time comparable with heavier alkali metals, such as Rb and Na, requires the design of a miniaturized trap. This is done by either a small-volume vacuum chamber and high currents [14] or a vacuum-compatible minitrap [15] which both increase the experimental complexity. Finally, even if the strong confinement is achieved, the scattering

length is still negative which prevents the formation of a stable BEC.

In this paper we show an all-optical way to condense  ${}^7\text{Li}$  atoms using tunable interatomic interactions. We use a 100-W ytterbium fiber laser to produce a  $\sim 2$ -mK potential well which traps  $\sim 10^6$  atoms from a magneto-optical trap (MOT). We explore two Feshbach resonances on the  $|F=1, m_F=0\rangle$  state and find that one of them is favorable for efficient forced evaporation starting directly from a phase-space density achieved in the MOT. We obtain a BEC on the  $|F=1, m_F=0\rangle$  internal state in less than 3 s of evaporation time.

## II. EXPERIMENTAL DETAILS

The  ${}^7\text{Li}$  atoms’ route to quantum degeneracy starts in an oven where they are heated up to  $450^\circ\text{C}$  to increase their vapor pressure. An atomic beam is collimated by two distant apertures and slowed down in an increased magnetic field Zeeman-slower. The capture velocity of the slower is set to  $\sim 800$  m/s.

Our MOT design and parameters are similar to that described in Ref. [16]. After a loading time of 3 s, the trap contains  $\sim 10^9$  atoms at a temperature of 1.2 mK. Trap lifetime, limited by a vacuum, is measured to be 10 s. The MOT parameters, such as pump and repump detunings and magnetic field gradient, are optimized to maximize the number of atoms. To improve the initial phase-space density we implement a so-called compressed MOT (CMOT) stage [16,17]. For 50 ms the laser intensities are attenuated, detunings are decreased, and the magnetic field gradient is increased. As a result the temperature is reduced to  $300\ \mu\text{K}$  and nearly half of the atoms are lost. By the end of this phase  $\sim 5 \times 10^8$  atoms are left in the trap with a density of  $n=4 \times 10^{11}$  atoms/cm<sup>3</sup> and a phase-space density of  $\rho=2 \times 10^{-5}$ .

The realization of the optical-dipole trap is shown in Fig. 1. A cw ytterbium fiber laser (IPG Fibertech) generates 100 W of linearly polarized light at  $1.07\ \mu\text{m}$  with a bandwidth of 2.83 nm. The first-order diffraction beam of an acousto-optic modulator (AOM), with 80% diffraction efficiency, is focused at the center of the MOT to a waist of  $31\ \mu\text{m}$ . The zeroth-order diffraction beam is only weakly focused to

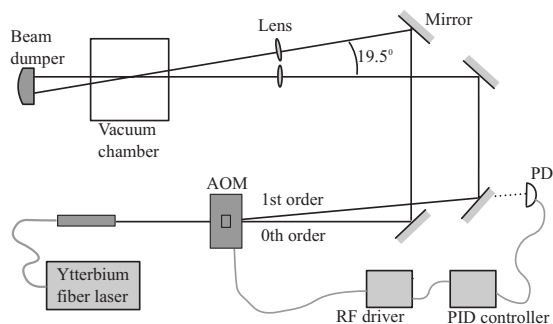


FIG. 1. A schematic representation of the optical-dipole trap experimental setup. The first-order diffraction beam is focused to a waist of  $31 \mu\text{m}$  and aligned to the MOT center. The zeroth-order beam is weakly focused to  $300 \mu\text{m}$ . It crosses the first-order beam at an angle of  $19.5^\circ$  and it only becomes important at the final stages of evaporation. AOM: acousto-optic modulator. PD: photodetector.

$300 \mu\text{m}$ , and it crosses the first-order beam at an angle of  $19.5^\circ$ . When maximum rf power is applied to the AOM this beam is very weak and it has no effect on the atoms. At full laser power (65 W in the trap region) the trap depth, produced by the first-order diffraction beam, is estimated to be  $\sim 2 \text{ mK}$ . Oscillation frequencies in the trap are predicted to be  $\omega_r = 2\pi \times 16 \text{ kHz}$  and  $\omega_z = 2\pi \times 120 \text{ Hz}$  for the radial and longitudinal directions, respectively. The radial oscillation frequency was measured by the parametric driving technique and found to be in excellent agreement with the predicted one. We keep the first-order diffraction beam at its full power throughout the MOT loading time, and atoms are loaded into the dipole trap mainly during the CMOT phase. Mechanical shutters are then used to block all resonant light from reaching the trapped atoms. The MOT pump beam, associated with the  $|F=2\rangle$  ground state, is blocked only a few milliseconds later to allow a 1-ms optical pumping pulse, effectively transferring all atoms into the  $|F=1\rangle$  ground state. Eventually, we are left with  $\sim 10^6$  trapped atoms. Phase-space density conditions are similar to those resulted from the CMOT phase.

We note that the loading efficiency of the optical trap from the CMOT is rather poor due to the small spatial overlap between the two traps. Even for 100 W laser power the high initial temperature of the  $^7\text{Li}$  atoms oblige a tight focusing of the beam in order to create a deep enough potential. This makes the use of a compressible crossed dipole trap to improve the loading conditions impractical [5].

### III. DETECTION OF FESHBACH RESONANCES ON THE $|F=1, m_F=0\rangle$ STATE

The scattering length of  $^7\text{Li}$  atoms on all sublevels and sublevel mixtures of the  $|F=1\rangle$  ground state at zero magnetic field is positive but very small ( $\sim 10a_0$ ), impeding efficient evaporation cooling. However, each sublevel and their mixtures possess at least one Feshbach resonance [18]. The resonance on the absolute ground state  $|F=1, m_F=1\rangle$  has been previously used for the final stage of forced evaporation in

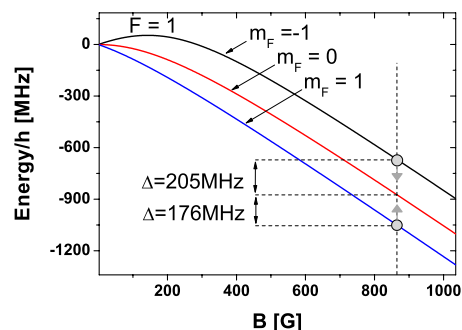


FIG. 2. (Color online) Energy-level splitting of the  $|F=1\rangle$  hyperfine state of  $^7\text{Li}$  atoms. With the presence of high magnetic fields, spin-flip collisions between  $|m_F=-1\rangle$  and  $|m_F=1\rangle$  states result in their transfer into  $|m_F=0\rangle$  with an excess of kinetic energy equal to  $h \times 29 \text{ MHz}$  ( $\sim K_B \times 1.4 \text{ mK}$ ).

an optical trap after precooling in a magnetic trap [19,20]. The resonances on other sublevels or their mixtures were neither reported nor used before.

The search for Feshbach resonances requires high offset magnetic fields. We use two pairs of Helmholtz coils that allow variable-bias fields of up to 1200 G. When the magnetic field is ramped up to high values we observe a  $\sim 50\%$  reduction in atom number. Our state-selective measurement shows that the remaining atoms are all on the  $|F=1, m_F=0\rangle$  state. We attribute this loss to spin-flip collisions between atoms on  $|F=1, m_F=-1\rangle$  and  $|F=1, m_F=1\rangle$  states. The energy-level splitting diagram of the  $|F=1\rangle$  state is shown in Fig. 2. A spin-flip collision that takes place at high magnetic fields flips the colliding atoms to the  $|F=1, m_F=0\rangle$  state and leaves them with an excess of kinetic energy equal to  $K_B \times 1.4 \text{ mK}$ , which is comparable to the trap depth. Most of the atoms escape, but we observe some increase in the  $|m_F=0\rangle$  population. Detection of losses and spontaneous spin polarization are the first manifestations of the increase in collisional cross section. As the  $|m_F=0\rangle$  state is stable against spin-exchange collisions at high magnetic fields, we search for signatures of Feshbach resonances on this state.

Figure 3(a) shows a theoretical prediction of the scattering length as a function of bias magnetic field. Two Feshbach resonances between 800 G and 900 G are indicated by the divergence of the scattering length. Experimentally, the resonances are usually observed by the detection of atom loss as in their proximity the inelastic collisional rate is strongly enhanced [21,22]. For this measurement we ramp up the magnetic field to different values in 40 ms and wait 0.5 s before decreasing it to 386 G in 40 ms where *in situ* state-selective absorption imaging is performed. In Fig. 3(b) the atom number as a function of bias magnetic field is shown. The atoms are initially prepared at a temperature of  $300 \mu\text{K}$ . Strong losses are observed around 830 G and 880 G featuring a narrow and a broad structure. By fitting them with simple Gaussian functions, a coarse estimation of the resonances locations and widths can be determined. According to the fit, the narrow resonance is  $7 \text{ G}$  wide ( $1/e^2$  radius) and it is located at  $831 \pm 4 \text{ G}$ . The uncertainty in its position is due to an uncertainty in the magnetic field calibration which is obtained by the detection of optical resonances and thus lim-

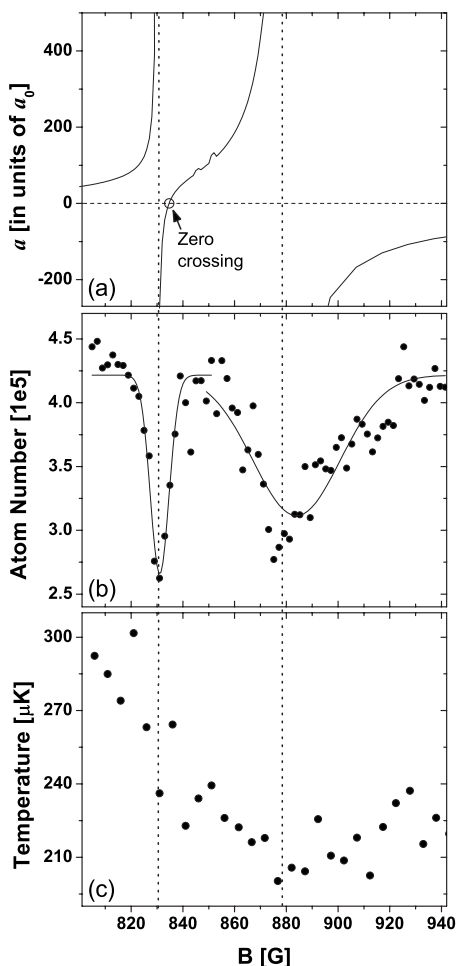


FIG. 3. (a) Theoretical predictions for the scattering length as a function of bias magnetic field in the  $|F=1, m_F=0\rangle$  state [18]. Divergence of the scattering length signify the presence of two Feshbach resonances. (b) The resonances are detected by measuring atom loss due to inelastic collisions. The solid lines are Gaussian fits to define the resonance positions. Note that the maximal loss does not coincide with the minimum of the Gaussian fit for the broad resonance. (c) Temperature of the atomic cloud in the optical trap as a function of bias magnetic field. Decrease in temperature indicates cooling by free evaporation.

ited by the linewidth of the excited states and the laser locking quality. The broad resonance located at  $884^{+4}_{-13}$  G is 34 G wide and features a notable asymmetric profile which tends to shift the center of a simple Gaussian fit to a higher magnetic field value as compared to the maximal loss position (detected at 875 G). Such an asymmetry in losses in the vicinity of broad Feshbach resonances has been recently reported for  $^{39}\text{K}$  atoms [23] and was attributed to a larger three-body loss coefficient from the negative-scattering-length side of the resonance and mean-field effects. The study followed of molecule association showed that the position of a broad Feshbach resonance is indeed shifted to a lower value [23]. Comparison between the experimental measurements [Fig. 3(b)] and the theoretical calculations [Fig. 3(a)] shows that the maximal loss position suits better the predicted distance between the two resonances. We there-

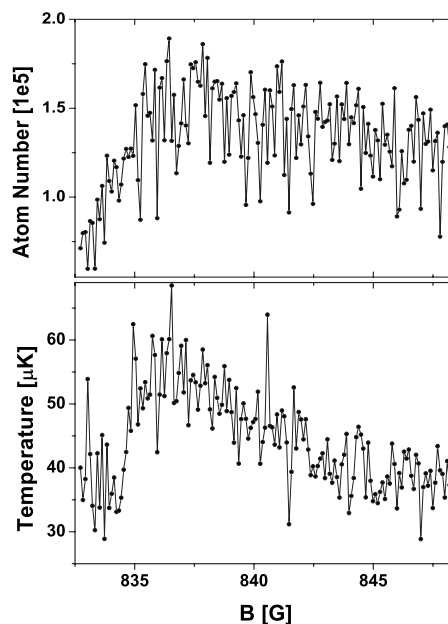


FIG. 4. The gain in atom number and increase in temperature, which indicate the lack of free evaporation cooling, reveal the zero crossing of the scattering length at  $836 \pm 4$  G.

fore believe that the actual location of the broad resonance is at a somewhat lower value than that given by the Gaussian fit and this systematic error increases the error bars of the experimentally detected resonance position.

Most excitingly, we observe an onset of free evaporation cooling together with the enhanced inelastic losses [Fig. 3(b)]. In Fig. 3(c) we show the temperature change as a function of the bias magnetic field. A decrease in the temperature indicates cooling which we attribute to the establishment of free evaporation when the collision rate becomes high enough. The observed cooling allows us to decrease the temperature by forced evaporation and then scan for Feshbach resonances, again to improve sensitivity.

We execute a short forced evaporation of 1.5 s, reducing the trap depth to 0.3 mK, 15% of its initial value. Evaporation is performed with a bias field of 850 G which is chosen to optimize the number-to-temperature ratio based on our scans for Feshbach resonances at high temperature [Figs. 3(b) and 3(c)]. By the end of this evaporation the atoms are cooled down to a temperature of  $\sim 50$   $\mu\text{K}$ . Our scan for inelastic losses in proximity to Feshbach resonances reveals the same positions of the resonances observed before including asymmetry in the profile of the broad resonance. However, an additional feature has been identified which we were unable to detect at high temperature. In Fig. 4, zero crossing of the scattering length manifests itself in terms of an increased temperature and number of atoms [24]. The hold time at high bias field for this experiment is 0.5 s. During this time efficient free evaporation reduces the temperature to 40  $\mu\text{K}$  if the collisional cross section is high enough. At zero crossing the scattering length vanishes and so does the cross section, impeding efficient free evaporation. The asymmetry in this measurement is caused by the proximity of the zero-crossing point to the narrow resonance at 831 G. The

zero-crossing point is detected at  $836 \pm 4$  G where the maximum temperature is observed.

#### IV. EVAPORATION COOLING TO THE BEC THRESHOLD

Forced evaporation cooling of the optically trapped atoms down to the BEC threshold is performed by attenuating the laser power, thus reducing the trap depth which scales linearly with the power reduction factor  $\alpha$ . A photodiode detector, located behind one of the mirrors, collects a fraction of the trap beam's power (see Fig. 1). It generates a voltage readout that is compared to a set-point signal by a PID controller. An error signal is fed back to the rf-power supplier of the AOM. With this scheme we are able to control trap depth reduction up to a factor of  $\alpha=3 \times 10^{-3}$ . As is well known, trap oscillation frequencies also decrease with the attenuation of laser power ( $\propto \sqrt{\alpha}$ ), affecting the rethermalization efficiency throughout the evaporation process. In addition to that, the strong bias magnetic field, employed during evaporation, creates a weak antitrapping potential in the longitudinal direction. This decreases further the optical confinement toward the end of the evaporation. Indeed, in a single-beam trap we were unable to cool atoms below a temperature of  $10 \mu\text{K}$ . The addition of a zeroth-order diffraction beam solves this problem. At the beginning of the evaporation it has no effect on the atoms as its potential depth is negligible. However, with the reduction of the first-order diffraction intensity, it strengthens to create a confinement potential to the atoms in the longitudinal direction of the trap. The longitudinal oscillation frequency, determined by the confining beam, is  $2\pi \times 60$  Hz. The zeroth-order beam can be effectively considered as a two-dimensional confining potential because it produces a very weak (0.14 Hz) oscillation frequency in its propagation direction which is easily overcome by the magnetic antitrapping potential. We note also that the crossed trap is slightly shifted from the location of the zeroth-order beam waist which reduces somewhat the potential at the end of the evaporation.

Forced evaporation is found to work most effectively when the bias field is set to 866 G. Based on the theoretical curve [Fig. 3(a)] we estimate the scattering length to be  $(300 \pm 100)a_0$ . The large uncertainty in the scattering length is due to the uncertainty in the position of the broad resonance. The trap depth is reduced exponentially in 3 s with a time constant of 330 ms to less than 0.5% of its initial value. In Fig. 5, *in situ* absorption imaging of the trapped atoms at 866 G reveals the onset of a BEC threshold by a familiar bimodal density distribution. The trace represents the atom longitudinal density after integrating the radial direction of the picture above it. Optical resolution is  $4 \mu\text{m}$ , less than the size of the BEC. The thermal atomic cloud is fitted with a Bose-Einstein distribution function which reveals a temperature of  $T=380 \pm 40$  nK. The total number of atoms is  $6 \times 10^3$  which sets the critical temperature to  $T_c=350$  nK. The fitting of the BEC with an inverted parabola reveals

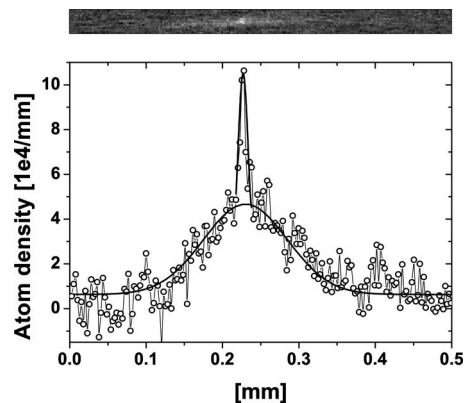


FIG. 5. Onset of BEC. *In situ* absorption imaging of atoms at the BEC threshold. The thermal atomic cloud is fitted with a Bose-Einstein distribution function which yields a temperature of  $380 \pm 40$  nK. The number of atoms in the BEC is  $\sim 700$ .

$\sim 700$  atoms in the condensate with a Thomas-Fermi radius of  $11 \mu\text{m}$ .

#### V. CONCLUSIONS

To conclude, we developed a method to all-optically condense  $^7\text{Li}$  atoms. This way facilitates the BEC production which is extremely demanding in magnetic traps. We observed a BEC with repulsive interactions on the  $|F=1, m_F=0\rangle$  state in less than 3 s of forced evaporation in a crossed-beam optical-dipole trap. We use the tunability of the interatomic interactions in the proximity of Feshbach resonances which we observed and characterized for this internal state.

We note that the condensate lifetime was very short (a few tenths of ms), presumably because of the extremely large scattering length. Moreover, our weak optical trap at the end of the evaporation was not stable enough due to the use of a single linear photodiode detector. A number of improvements can be implemented to optimize the performance of the described method. Better laser beam stability, which can be achieved by using either two detectors [7] or a logarithmic detector, and a decrease of the scattering length toward the end of evaporation will improve the condensate lifetime. An improved vacuum would allow an increase in the number of atoms in the condensate.

#### ACKNOWLEDGMENTS

We thank S. Kokkelmans for providing us with theoretical calculations of Feshbach resonances on all sublevels of the  $^7\text{Li}$  lower hyperfine state. This work was supported, in part, by the Israel Science Foundation, through Grant No. 1125/04.

- [1] M. D. Barrett, J. A. Sauer, and M. S. Chapman, *Phys. Rev. Lett.* **87**, 010404 (2001).
- [2] Y. Takasu, K. Maki, K. Komori, T. Takano, K. Honda, M. Kumakura, T. Yabuzaki, and Y. Takahashi, *Phys. Rev. Lett.* **91**, 040404 (2003).
- [3] T. Weber, J. Herbig, M. Mark, H.-C. Nägerl, and R. Grimm, *Science* **299**, 232 (2003).
- [4] S. R. Granade, M. E. Gehm, K. M. O'Hara, and J. E. Thomas, *Phys. Rev. Lett.* **88**, 120405 (2002).
- [5] T. Kinoshita, T. Wenger and D. S. Weiss, *Phys. Rev. A* **71**, 011602(R) (2005).
- [6] R. Dumke, M. Johanning, E. Gomez, J. D. Weinstein, K. M. Jones, and P. D. Lett, *New J. Phys.* **8**, 64 (2006).
- [7] J. Fuchs, G. J. Duffy, G. Veeravalli, P. Dyke, M. Bartenstein, C. J. Vale, P. Hannaford, and W. J. Rowlands, *J. Phys. B* **40**, 4109 (2007).
- [8] E. Timmermans, P. Tommasini, M. Hussein, and A. Kerman, *Phys. Rep.* **315**, 199 (1999).
- [9] R. A. Duine and H. T. C. Stoof, *Phys. Rep.* **396**, 115 (2004).
- [10] J. Söding, D. Guéry-Odelin, P. Desbiolles, G. Ferrari, and J. Dalibard, *Phys. Rev. Lett.* **80**, 1869 (1998).
- [11] C. C. Bradley, C. A. Sackett, J. J. Tollett, and R. G. Hulet, *Phys. Rev. Lett.* **75**, 1687 (1995).
- [12] E. R. I. Abraham, W. I. McAlexander, J. M. Gerton, R. G. Hulet, R. Côté, and A. Dalgarno, *Phys. Rev. A* **55**, R3299 (1997).
- [13] J. Dalibard, in *Bose-Einstein Condensation in Atomic Gases*, Proceedings of the International School of Physics "Enrico Fermi," Course CXL, edited by M. Inguscio, S. Stringari, and C. Wieman (IOS Press, Amsterdam, 1999).
- [14] F. Schreck, G. Ferrari, K. L. Corwin, J. Cubizolles, L. Khaykovich, M.-O. Mewes, and C. Salomon, *Phys. Rev. A* **64**, 011402(R) (2001).
- [15] R. Wang, M. Liu, F. Minardi, and M. Kasevich, *Phys. Rev. A* **75**, 013610 (2007).
- [16] U. Schünemann, H. Engler, M. Zielonkowski, M. Weidemüller, and R. Grimm, *Opt. Commun.* **158**, 263 (1998).
- [17] M.-O. Mewes, G. Ferrari, F. Schreck, A. Sinatra, C. Salomon, *Phys. Rev. A* **61**, 011403(R) (1999).
- [18] S. J. J. M. F. Kokkelmans (private communication).
- [19] L. Khaykovich, F. Schreck, G. Ferrari, T. Bourdel, J. Cubizolles, L. D. Carr, Y. Castin, and C. Salomon, *Science* **296**, 1290 (2002).
- [20] K. E. Strecker, G. B. Partridge, A. G. Truscott, and R. G. Hulet, *Nature (London)* **417**, 150 (2002).
- [21] P. O. Fedichev, M. W. Reynolds, and G. V. Shlyapnikov, *Phys. Rev. Lett.* **77**, 2921 (1996).
- [22] S. Inouye, K. B. Davis, M. R. Andrews, J. Stenger, H.-J. Miesner, D. M. Stamper-Kurn, and W. Ketterle, *Nature (London)* **392**, 151 (1998).
- [23] C. D'Errico, M. Zaccanti, M. Fattori, G. Roati, M. Inguscio, G. Modugno, and A. Simoni, *New J. Phys.* **9**, 223 (2007).
- [24] K. M. O'Hara, S. L. Hemmer, S. R. Granade, M. E. Gehm, J. E. Thomas, V. Venturi, E. Tiesinga, and C. J. Williams, *Phys. Rev. A* **66**, 041401(R) (2002).